Article in Press

Fire removes preexisting pyrogenic organic matter from the ecosystem through the mechanisms of both direct combustion and increasing mineralizability

Mengmeng Luo[1] · Kara Yedinak[2] · Keith Bourne[3] · Thea Whitman[1,4]

Received: 19 March 2026 / Accepted: 4 October 2026
© The Author(s) 2026

Abstract

Pyrogenic organic matter (PyOM) produced during fires plays an important role in the global carbon (C) cycle due to its low microbial availability and resulting high persistence. However, PyOM can be combusted or chemically altered in subsequent fires. To explore the effects of subsequent fire on PyOM, we used a mass loss calorimeter to simulate reburning by delivering realistic heat fluxes to jack pine (*Pinus banksiana* Lamb.) PyOM produced at 350 °C. We tested three heat flux profiles (High, Low, and Control) and three burial depths (Surface, 1 cm, and 5 cm) arranged in a full-factorial design, with the "high" heat flux profile consisting of heating for 4.72 h with a peak of 85 kW m^{-2} and "low" heating for 2.5 h with a peak of 45 kW m^{-2}. We found that both variables affected the C remaining after the simulated reburn ($p < 0.05$), with greater C losses at higher heat fluxes and shallower exposure depths. Consistent with our predictions, treatments with high heat exposure (HF_{High} + Surface, HF_{High} + 1 cm, HF_{Low} + Surface) showed increases in pH and decreases in total dissolved organic carbon (DOC) and mineralized C after the simulated reburn. Counter to our predictions, treatments with intermediate reburn conditions (HF_{High} + 5 cm and HF_{Low} + 1 cm) caused decreases in pH and increases in DOC, mineralized C, modelled decomposable C, and modelled C decomposition rate ($p < 0.05$), compared to the unburned controls. These findings highlight that, despite its high persistence in fire-free conditions, PyOM can also be readily combusted and altered in subsequent fires, with important implications for changing fire regimes and the global C cycle.

Synopsis

Subsequent fires, represented by simulated reburns with realistic heat fluxes, not only consume PyOM produced in previous burns, but can also increase its susceptibility to microbial decomposition, which challenges the potential for PyOM to contribute to long-term carbon storage.

Responsible Editor: Lettice Hicks

This Article in Press is shared early to give you faster access to new research. It is citable and carries a permanent DOI. The final edited version will replace it automatically.

https://doi.org/10.1007/s10533-026-01380-6

Published online: 17 October 2026

Keywords Pyrogenic organic matter · Pyrogenic carbon · Mineralizability · Dissolved organic carbon · Carbon decomposition · Subsequent fire · Simulated reburn

Introduction

As the second largest pyrogenic carbon (PyC) pool in the world, after marine sediments (Bird et al. 2015; Santín et al. 2016), soil PyC is an important component of global carbon (C) stocks. Soil PyC, which can comprise less than 1% to over 45% of total soil organic carbon (SOC) (Forbes et al. 2006), varies across and within ecosystems, influenced by factors such as land cover, land use, climate, and topography (Abney and Berhe 2018). Pyrogenic carbon is a constituent of pyrogenic organic matter (PyOM)—the dark-colored, carbon-rich residue produced during incomplete combustion of organic matter (Keiluweit et al. 2010; Zimmerman and Mitra 2017; Bartoli et al. 2021). Pyrogenic organic matter is often characterized by a high degree of aromatic condensation (Preston and Schmidt 2006; Matosziuk et al. 2019), which contributes to its relatively high persistence compared to uncharred organic matter, with a mean turnover time ranging from decades to thousands of years (DeLuca and Aplet 2008; Major et al. 2010; Knicker 2011).

However, PyOM is chemically heterogeneous (Keiluweit et al. 2010; Boot et al. 2014; Bird et al. 2015) and is certainly not inert. The fate of soil PyOM is influenced by physical, chemical, and biological processes. Its stability is governed by both its intrinsic chemical properties and interactions with the surrounding environment (Knicker 2011; Heitkötter and Marschner 2015; Abney et al. 2019). Yet, despite growing recognition of its ecological significance, the mechanisms regulating the persistence, transformation, and mobility of PyOM in soil remain insufficiently characterized (Berhe et al. 2007; Singh et al. 2012; Soucémarianadin et al. 2019).

To characterize the mechanisms that control PyC dynamics, we can turn to the classic soil-forming processes: additions, losses, transformations, and translocations (Simonson 1959). Each of these processes is significantly influenced by fire, which is naturally a dominant force in PyC cycling (Preston and Schmidt 2006; Santín et al. 2016) and is even proposed to represent a soil-forming factor in itself (Certini 2013). Thus, we must also consider each process in the context of "subsequent fire". Over sufficiently long timescales, almost every fire occurs within the footprint of a previous one. However, patterns of fire activity have been dramatically altered by human influence. In North America, fire exclusion following European settlement disrupted historical fire regimes (Nikolakis and Roberts 2020), while ongoing rising temperatures and increasing drought events have led to greater fire frequencies in many regions (Westerling et al. 2006; Bowman et al. 2009; Mansoor et al. 2022). As a result, fires are now more likely to recur in the same location within ecologically relevant timescales. We refer to these as "subsequent fires" –sometimes termed *reburns* or *repeated fires* in the literature – (Bartoli et al. 2021; Saberi and Harvey 2023), and within the context of subsequent fires, we consider the four processes governing the fate of PyOM in soil.

Additions

Fire is the dominant natural process responsible for generating new inputs of PyOM in terrestrial ecosystems. Through pyrolysis, fire transforms plant biomass, litter, and soil organic matter (SOM) into PyOM, thereby contributing to the persistent C pool (Ohlson et al. 2009; Abiven and Santín 2019). The quantity and properties of PyOM produced can vary with combustion conditions and fuel characteristics (Doerr et al. 2018; Abiven and Santín 2019). PyC formed under higher-heat conditions generally exhibits greater resistance to degradation than PyC formed under lower-heat conditions (Preston and Schmidt 2006; Keiluweit et al. 2010; Doerr et al. 2018).

Spatial and temporal variation in fire regimes also influences PyOM additions across ecosystems. For instance, frequently burned grasslands may contribute smaller PyOM inputs during individual fire events than ecosystems characterized by less frequent but larger fire events, although their cumulative contributions over time can be substantial (Soong and Cotrufo 2015). In contrast, infrequent fires in systems with greater fuel accumulation may

generate relatively large PyOM inputs during individual fire events, although longer vegetation recovery periods can limit the frequency of subsequent additions (Santín et al. 2015; Coppoletta et al. 2016) (Fig. 1a). Thus, PyOM addition rates are closely linked to fire regime characteristics, including fire frequency, combustion conditions, and postfire vegetation recovery dynamics.

Losses

Pyrogenic carbon can be removed from terrestrial ecosystems through both rapid and gradual pathways (Fig. 1b). One rapid loss pathway is combustion during subsequent fires, in which preexisting PyC is further oxidized to carbon dioxide (CO_2). Under sufficiently high fire intensity, surface and near-surface PyC may be partially or completely combusted, resulting in substantial reductions in PyC stocks (Preston and Schmidt 2006; Santín et al. 2013).

In contrast, post-fire losses of PyC are considerably slower but long-lasting, with rates decreasing as production temperature increases (Kasin and Ohlson 2013; Abney et al. 2019). Chemical and biological oxidation are common mechanisms that lead to PyC loss over time (Bruun et al. 2008; Leuthold et al. 2025). Chemical oxidation, often mediated by oxygen-rich environments or abiotic reactions, can also enhance microbial access to PyC (Kasin and Ohlson 2013). Microbial decomposition, especially by heterotrophic communities, can slowly mineralize PyC to CO_2 (Major et al. 2010; Abney et al. 2019; Johnson et al. 2023), though this pathway typically acts more readily on less condensed or partially charred fractions. While the rates for post-fire losses are low compared to the rate of combustion losses, they play an important role in long-term PyC turnover (Santos et al. 2012; Singh et al. 2012) and can also influence non-pyrogenic soil C cycling (Maestrini et al. 2015; Whitman et al. 2026).

Transformation

The transformation of PyOM during subsequent fires depends not only on reburn conditions, but also on the characteristics of the preexisting PyOM. The degree of condensation and aromaticity can determine whether PyOM is susceptible to further alteration or largely resistant (Abney et al. 2019). When exposed to fire again, the outcome is also strongly shaped by oxygen availability and heating intensity. Under aerobic conditions, PyOM

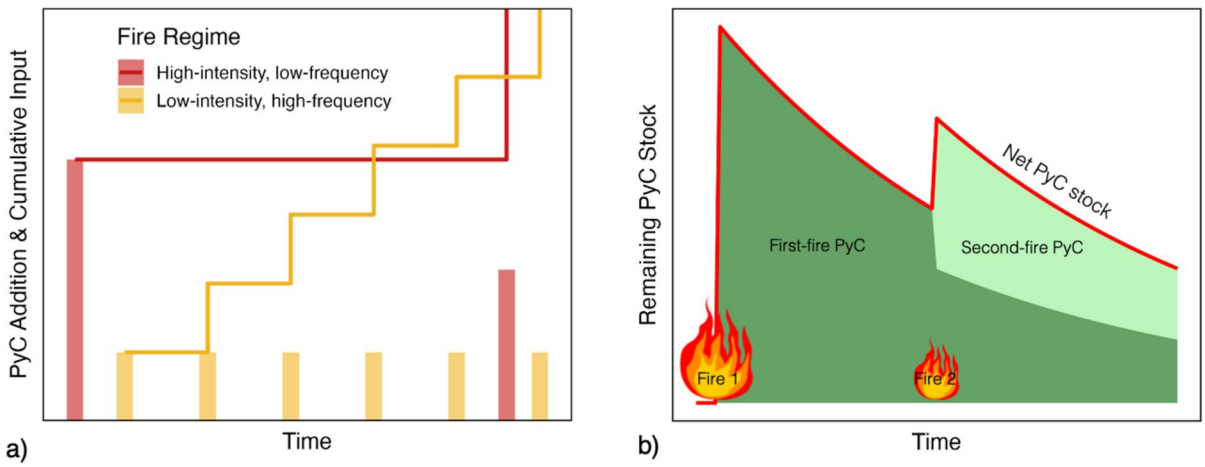


Fig. 1 Conceptual illustration of fire effects on PyC dynamics. **a** PyC additions with individual fire events (bars) and cumulative PyC inputs (step lines) over time under contrasting fire regimes. **b** Net PyC stock over time with recurrent fires, showing the contributions from first- and second-fire PyC pools (dark and light green, respectively) when both PyC additions and losses are considered. The red line indicates the net PyC stock over time. (Illustrating conceptual trends, not to scale)

may lose residual pyrolysis-derived volatile and condensed compounds trapped within pore structures, thereby exposing previously occluded pore space, increasing surface area and reactivity, and enhancing microbial accessibility (Xiao 2022). In contrast, under anoxic or pyrolytic conditions, condensed structures can be preserved or even further stabilized, increasing resistance to subsequent decomposition (Spokas 2010).

Beyond fire-driven events, PyOM also undergoes gradual transformation over ecological timescales. Abiotic processes such as physical fragmentation and chemical oxidation, as well as microbial metabolism, can reduce aromaticity and modify surface chemistry (Preston and Schmidt 2006; Dungait et al. 2012). Some relatively labile PyC fractions may be assimilated by microbes and subsequently stabilized in microbial biomass or necromass, thereby shifting them into different persistent C pools (Bruun et al. 2008; Kuzyakov et al. 2009; Sokol et al. 2022).

Translocations

During a fire, a small portion of PyC is emitted as aerosol black carbon (0.5–1.8% of the on-site PyC production per year), which can be transported by wind and later deposited (Bird et al. 2015; Santín et al. 2016). However, the majority of PyC typically remains on the surface or in the soil, where it can be translocated through both lateral (e.g., surface run-off, aeolian transport) and vertical (e.g., leaching, bioturbation) pathways. These post-fire PyC movements remain poorly quantified (Bird et al. 2015; Santín et al. 2016; Abney and Berhe 2018).

As with total SOC, PyC concentration typically decreases with soil depth and has a strong positive correlation with total SOC concentration (Matosziuk et al. 2020). Evidence also suggests that PyC may be preferentially transported downward relative to other forms of SOC (Soucémarianadin et al. 2019). Additionally, small particle sizes (< 53 μm) or bigger surface areas facilitate the adsorption of PyC onto fine soil particles and enhance downward movement (Ansley et al. 2006; Pingree and DeLuca 2017). Finer, older, and more aromatic PyC is often found in deeper soil profiles, suggesting that water percolation, interacting with other transformation processes, contributes to vertical redistribution over time (Hobley 2019; Soucémarianadin et al. 2019). However, downward migration of PyC is slow in nature and may be inhibited by fire-induced hydrophobicity, which limits water infiltration (Huffman et al. 2001), at least in the short term post-fire.

Lateral transport also plays an important role, particularly through post-fire erosion. Water and wind can relocate PyOM from its point of origin and deposit it in topographic depressions (Tinner et al. 2006), water bodies, or seasonally flooded anaerobic sites, thereby reducing microbial decomposition and enhancing persistence (Berhe et al. 2007). In rare cases, such depositional events, especially burial by loess, can preserve PyC for millennia in deep, oxygen-limited environments (Marín-Spiotta et al. 2014).

Despite these potential pathways, the majority of PyC tends to remain near the soil surface. Over decadal timescales, more than 70% is found in the top 10 cm, and most within the top 30 cm (Carcaillet 2001; Gavin 2003; Silva et al. 2023). In shorter-term studies following recent PyOM deposition, PyC is typically concentrated in the top 15 cm (Major et al. 2010; Foereid et al. 2011). These consistent surface accumulations highlight the relatively low mobility of PyC under most field conditions, despite the range of processes that can facilitate its translocation.

Together, additions, losses, transformations, and translocations control the size and nature of PyC stocks in soils, and are, in turn, influenced by subsequent fire. Changes in the Anthropocene further increase the need to understand how PyC produced during one fire is affected by a subsequent fire in the context of these processes. In a previous companion study, we designed a system to deliver realistic heat fluxes to a pyrocosm to simulate subsequent fire effects on PyOM in a sand matrix (Luo et al. 2025). Building on this system, our present study addresses the central question: How does subsequent fire influence the chemical properties (transformation) and the microbial decomposition (losses) of the preexisting PyC (Fig. 2)?

This study focuses on three main aspects of PyC persistence during and after reburns: 1) protection through burial at different depths (effects of previous translocations); 2) changes in potential for leaching and microbial availability, assessed via dissolved organic carbon (DOC) (transformations); and 3) changes in biological degradation, assessed through cumulative C mineralization (losses). We hypothesized that the combination of different

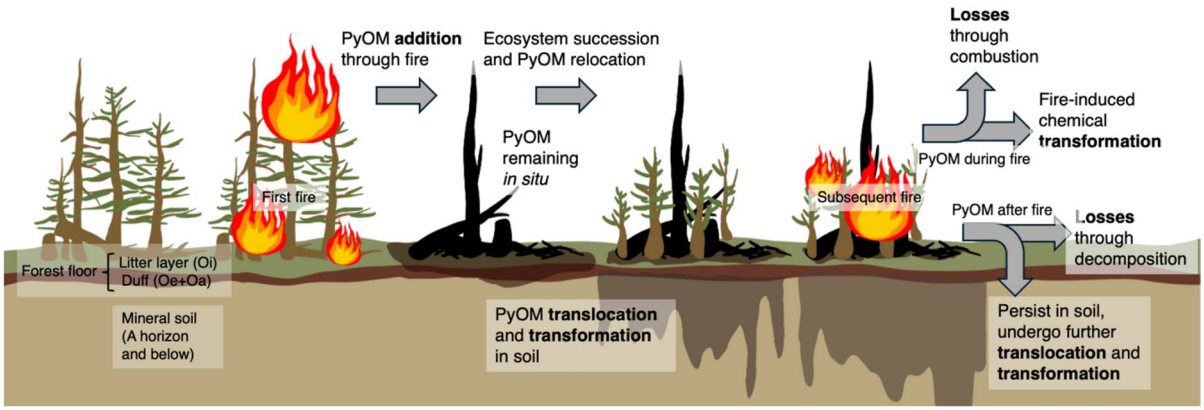


Fig. 2 Conceptual diagram illustrating our central research question: What will happen to PyOM during and after a second fire? After the first fire, the residual PyOM on the forest floor decreases due to translocation and microbial degradation. Some PyOM percolates into mineral soil with water and biological activity and is deposited deeper in the soil profile (Major et al. 2010; Bird et al. 2015; Santín et al. 2016). This diagram drew inspiration from Fig. 2 in Santín et al. (2016)

heat fluxes (HFs) and depths would influence pH, total C content, DOC, and the mineralized C of the PyOM in the simulated reburn. Higher HFs and shallower burial depths were expected to result in higher pH, due to greater ash deposition on and near the surface. However, these same conditions would lead to lower total C, mineralized C, and DOC, reflecting increased thermal degradation and reduced microbial accessibility.

Materials and methods

We designed our system to represent a jack pine-dominated pine barrens (*Pinus banksiana* Lamb.) characteristic of northwestern Wisconsin, USA. Pine barrens typically have well-drained to excessively well-drained sandy soils, and the natural fire return interval for jack pine stands in the area is 3–7 years (Radeloff et al. 2004), generally with low fire severity. We produced PyOM from jack pine wood (77.8% C) using a modified muffle furnace (Güereña et al. 2015) under an argon atmosphere at 350 °C for 30 min (Luo et al. 2025), using wood from the trunk of a small jack pine tree from Wilson State Forest Nursery (43.1461124, − 90.6950388). Before pyrolysis, the wood was dried and milled < 2 mm to support even pyrolysis throughout.

We simulated the effects of fire using the method described in detail in Luo et al. (2025). Briefly, we used a mass loss calorimeter to expose PyOM to high and low heat fluxes (HF_{High} and HF_{Low}) at the surface, buried 1 cm, and buried 5 cm deep in an ashed sand matrix ("pyrocosm"), chosen to represent the typically sandy soil of jack pine forests. The dynamic high (heating for 4.72 h with a peak of 85 kW m^{-2}) and low (heating for 2.5 h with a peak of 45 kW m^{-2}) heat fluxes, representing different heat received on the soil surface, were parameterized using data from log burns (Luo et al. 2025). The high and low heat flux profiles represent surface fire generated from the burning of downed wood, distinguished by different fuel load and continuity (Luo et al. 2025). For each depth and heat treatment, we had five individual replicates, which were exposed to the same heat flux (or control) at the same time, but were distanced from each other during exposure and then analyzed individually (Fig. S1.1). Thus, there were nine pyrocosms in total—one for each combination of heat flux and depth treatments, with five replicates within each pyrocosm. For each replicate, 1 g PyOM was mixed with 8 g sand, and buried or placed at the surface in the shape of a cylinder 30 mm in diameter and 16 mm thick. Samples were situated at the surface or buried in the pyrocosm at the appropriate depth using a 3D-printed polylactic acid (PLA) sample placer (modeled with Tinkercad; printed with Ultimaker S5, University of Wisconsin-Madison Makerspace). Temperatures during this study were tracked using type K thermocouples (Omega Engineering, GG-K-30-SLE) positioned at the bottom of each sample and recorded with LabVIEW (National Instruments 2013) (Luo et al. 2025). We

measured chemical parameters including pH, total C, and DOC, and evaluated biological C mineralization, to test how different heat exposures affect the chemical and biological properties of PyOM during a simulated reburn.

Sample collection, unified dilution, and homogenization

To ensure we captured as much of the PyOM as possible, we collected and analyzed it as a PyOM-sand mixture, rather than trying to physically separate the PyOM from the sand matrix. By analyzing blank sand along with sand-PyOM mixtures, we can infer the properties of PyOM without overlooking tiny particles that are difficult to retrieve, or soluble components that would be lost if we had used a water or other density-based extraction. For the total elemental analyses, this decision should have no effect on our calculation of stocks. For the pH measurements, the presence of sand presumably influenced the absolute pH values (compared to pure PyOM). However, we expect treatment comparisons to remain robust despite the dilution of PyOM with sand. Similarly, for C mineralization assays, absolute rates would be expected to differ from those that would have been obtained incubating pure PyOM, but the relative treatment effects are expected to remain consistent.

All PyOM-sand matrix samples were collected from the pyrocosm after undergoing sufficient cooling to be safe to handle and after pyrocosm/treatment mass loss recording. Surface samples were retrieved directly; for 1 cm and 5 cm samples, before retrieval, the sand on the top was carefully scraped away down to just above the depth of the samples. After the PyOM retrieval, we used a custom-designed 3D-printed PLA sample divider (Fig. S1.2) to collect the rest of the sand (along with any trace amounts of remaining PyOM) in the pyrocosm. The sample divider includes a sharp cutting end with five wedges (with interior angle of 72°) that allows it to evenly separate the samples by cutting through the sand to the bottom of the pyrocosm. Then we flipped the divider and the pyrocosm together. The collection area at the other end has five identical chambers to hold the sand in individual sections for each replicate (Fig. S1.2), so the sand drops into each chamber. To retrieve the sand from each chamber, we poured the sand out from one chamber while covering the other chambers at the same time. For the unburned controls, PyOM was buried as for the burn treatments, and then retrieved using the same processes as for the burned samples.

After sample collection, each PyOM-sand sample was weighed individually. To ensure a consistent sand mass across samples, we first estimated the PyOM mass remaining within each sample based on the mean mass loss observed among the fire replicates in each pyrocosm (assuming the mass loss for the whole pyrocosm is m, then the mean mass loss is $\frac{m}{5}$ for each individual sample). Then we used reserved sand from the corresponding section of the pyrocosm where each sample was located to bring the final mass of sand to 80 g for each sample. Thus, all final samples had 80 g sand mixed with whatever mass of PyOM out of the initial 1 g remained. For further analysis, each sample ($n = 45$) was ground and homogenized individually in Fritsch Vibrating Cup Mill Pulverisette 9 (FRITSCH GmbH – Milling and Sizing, Idar-Oberstein, Germany) at 1500 rpm for 10 s. We also homogenized a subsample of ashed and washed sand, which was used as the sample blank for subsequent analyses. All of the following analyses were done using these ground and homogenized samples.

Measuring pH

For each sample (PyOM-sand mixture) and the sample blank (ground quartz sand), 0.5 g was weighed in a 15 mL Falcon tube and saturated with 0.5 mL of deionized (DI) water for 48 h before the measurement. Because the samples were dry, the initial addition of water likely initiated various chemical reactions within the sample that led to unstable pH values immediately after wetting-up. To allow the sample to equilibrate at a stable pH, we let them sit for 48 h before measuring pH. Ecologically speaking, this wet-up process could roughly represent the first rain after a fire. After the equilibration, another 9.5 mL of water was added to each tube, bringing the solid (g) to liquid (mL) ratio to 1:20, following Zeba et al. (2022). Then all tubes were oscillated in an INCU-SHAKER 10L (Benchmark Scientific, Sayreville, NJ, USA) for 10 min at 200 rpm and centrifuged with a Centrifuge 5810 R (15 amp version, Eppendorf, Hamburg, Germany) at 3214 rcf for 15 min. Two lab replicates of 1 mL of the

supernatant solution were extracted from the tube for each sample and measured with a pH electrode InLab Micro (Mettler Toledo, Columbus, OH, USA) connected to a Thermo Scientific Orion Star A215 pH/Conductivity Meter (Thermo Fisher Scientific, Waltham, MA, USA). Lab replicates were subsequently averaged.

Total carbon

Samples used for measuring total C were dried at 60 °C for 48 h before preparation. Samples were wrapped in CE Elantech 5 × 9 mm tin capsules (~60 mg, for treatments HF_{High} + 5 cm, HF_{Low} + 1 cm, HF_{Low} + 5 cm, and controls) and 10 × 12 mm tin capsules (200–400 mg, for treatments HF_{High} + Surface, HF_{High} + 1 cm, and HF_{Low} + Surface, which had lower C concentrations) and analyzed using a Thermo Flash EA 1112 NC Analyzer (Thermo Fisher Scientific, Waltham, MA, USA) at the Jackson Lab, UW-Madison (Madison, WI, USA). Two lab replicates were analyzed for each sample and averaged. Total C is presented as C stocks (mg of C per sample).

Dissolved organic and inorganic carbon

Dissolved organic carbon samples were prepared with a 1:3 sample-to-water ratio using DI water (7 g sample with 21 mL DI water). Samples were oscillated at 150 rpm for 60 min and centrifuged at 2000 rcf for 10 min (Jones and Willett 2006; Hofmann et al. 2012). The supernatant of the solution was extracted with a syringe and filtered through the GD/X 25 mm Sterile Syringe Filter (glass microfiber filtration medium, 0.45 µm) into 17 mL TOC tubes (ashed at 450 °C for 8 h in a muffle furnace to remove any trace C). All samples were analyzed within 24 h of the extraction and stored at 4 °C before analysis. Total dissolved carbon (TC) and dissolved inorganic carbon (DIC) were measured by combustion using a Sievers M5310 C Laboratory TOC Analyzer System with GE Autosampler (General Electric, Boston, MA, USA) at the Water Science and Engineering Laboratory, UW-Madison (Madison, WI, USA). Dissolved organic carbon was calculated by subtracting DIC from TC. The raw DOC data were translated into units of "mg DOC per PyOM-sand sample" using Eq. (1),

$$DOC = C_{DOC} \cdot \frac{V}{m} \cdot M \tag{1}$$

where C_{DOC} is the concentration of DOC in mg L^{-1}, which is the direct measurement from the equipment. m is the mass of sample (7 g) that is used for DOC extraction. V is the volume of DI water added to sample (0.021 L). M is the total mass (~80 g) of each sample. DIC was also calculated with the same equation.

Twelve-week incubation

To investigate PyC mineralization after the simulated reburn, we incubated samples for 12 weeks with a microbial inoculum. The setup for the 12-week incubation was comprised of a vial of 15 g sample with microbial inoculant added and a vial of potassium hydroxide (KOH) solution (the CO_2 trap) placed inside a sealed 8 oz (236.6 mL) glass jar (Burch Bottle and Packaging, Queensbury, NY, USA) (Schindelbeck et al. 2016). All samples, along with 3 sample blanks (ground quartz sand) were included in the incubation, subtracting the blank values from the sample values for the incubation data.

We inoculated each sample with a microbially active soil extraction along with a nutrient solution, with the aim of avoiding nutrient limitation and focusing on C mineralizability. The inoculant for the sample incubation was composed of a microbial extraction from a previously burned soil, collected in 2020, six years after the 2014 King Fire (38.86953, − 120.61322) in California (Zeba et al. 2023). The soil is a sandy clay loam, with a pH of 5.7. With all treatments receiving the same inoculum source, our primary interest was in relative differences in PyOM mineralizability among treatments rather than absolute mineralization rates under field-specific microbial communities. After the soil was retrieved from the − 23 °C freezer and thawed at 4 °C, 5 g of the soil was incubated at 25 °C in a VWR Incubator Gr Con 4CF (Thermo Electron, Langenselbold, Germany) at 60% water holding

capacity (WHC) for 8 days in order to reactivate the microbial community (Whitman et al. 2013). This resulting community would of course not be expected to perfectly mimic a natural soil microbial community—rather, our goal was to derive a complex community that would be likely to have natural abilities to degrade PyOM, given its recent fire history.

To create the inoculum, 4.5 g incubated soil was added to 225 mL of DI water (1:50 w/v) and shaken at 100 rpm for 30 min. Then the solution was left to settle for 10 min and filtered through Whatman 1 filter paper. This extract was mixed with a nutrient solution in a 500 mL volumetric flask (with DI water added to 500 mL). The resulting 500 mL nutrient-inoculant solution contained the microbial extract, 4 mmol L^{-1} ammonium nitrate (NH_4NO_3), 4 mmol L^{-1} calcium chloride ($CaCl_2$), 2 mmol L^{-1} potassium dihydrogen phosphate (KH_2PO_4), 1 mmol L^{-1} potassium sulfate (K_2SO_4), 1 mmol L^{-1} magnesium sulfate ($MgSO_4$), 25 µmol L^{-1} boric acid (H_3BO_3), 2 µmol L^{-1} manganese sulfate ($MnSO_4$), 2 µmol L^{-1} zinc sulfate ($ZnSO_4$), 2 µmol L^{-1} iron(II) chloride ($FeCl_2$), 0.5 µmol L^{-1} copper sulfate ($CuSO_4$), and 0.5 µmol L^{-1} sodium molybdate (Na_2MoO_4) (Cheng et al. 2006; Whitman et al. 2013).

Each 15 g PyOM-sand sample received 2.05 mL of nutrient-inoculant solution, representing 55% WHC, and was placed in the larger glass jar. 5 mL of CO_2-depleted DI water was added to the bottom of each jar to maintain a moist environment during the incubation (Whitman et al. 2014). Each jar received a vial with 15 mL 0.05 mol L^{-1} KOH to serve as the CO_2 trap, and was sealed for incubation at 25 °C in a VWR Incubator Gr Con 4CF (Thermo Electron, Langenselbold, Germany).

For each sample, the vial of KOH solution was retrieved and replaced with a new vial of KOH solution 2, 4, 8, and 12 weeks after the start of the incubation. At each retrieval, the electric conductivity (EC) of the KOH vial was measured with an Orion DuraProbe Conductivity Probe connected to the Orion Star A215 pH/Conductivity Meter (Thermo Fisher Scientific, Waltham, MA, USA). The EC of the new KOH solution was also recorded at the beginning of the incubation and during each retrieval.

The KOH trap is used because KOH reacts with CO_2 to produce potassium carbonate (K_2CO_3) (Eq. 2), which causes a linear change in EC. Based on the change of EC, we can calculate how much CO_2 is emitted (Whitman et al. 2014; Eq. 3).

$$2KOH + CO_2 \rightarrow K_2CO_3 + H_2O \tag{2}$$

We also ran a separate "abiotic incubation" to evaluate how much CO_2 is emitted from the dissolution of inorganic C (especially for the treatments with higher ash production) in the PyOM-sand samples. This set of incubation trials was inoculated with only nutrient solution and water filtered through a 0.2 µm cellulose acetate sterile syringe filter to minimize the potential for contamination by microbes.

Carbon mineralization

The calculation of C loss as CO_2 (CO_2-C, in mg) in each PyOM-sand sample follows Eq. 3 (Strotmann et al. 2004; Schindelbeck et al. 2016; Johnson et al. 2023),

$$CO_2 - C = \frac{\frac{EC_{raw}-EC_{fin}}{EC_{raw}-EC_{sat}} \cdot V \cdot C_{KOH} \cdot A \cdot M_{CO_2} \cdot \frac{M_C}{M_{CO_2}}}{m_s} \cdot m_t \cdot 1000 \tag{3}$$

where EC_{raw} is the EC measured for pure 0.05 mol L^{-1} KOH. EC_{sat} is the EC measured for 0.025 mol L^{-1} K_2CO_3 (the result when all OH ions have reacted with CO_2). EC_{fin} is the EC measured at each retrieval. V is the volume of the KOH trap in liters (0.015 L). C_{KOH} is the molarity of the KOH trap (0.05 mol L^{-1}). A is the ratio of CO_2 needed to react with one portion of KOH (0.5). M_{CO_2} is the molar mass of CO_2 (44.01 g mol^{-1}). M_C is the molar mass of C (12.011 g mol^{-1}). m_s is the mass of sample used for incubation (~ 15 g). m_t is the total sample mass for each sample (~ 80 g). Measurements from the sample blanks (quartz sand with inoculant) were averaged and

deducted from each sample to account for CO_2 present in the jars when they were sealed and any trace amounts of C from the quartz sand and inoculant itself.

In order to compare the relative mineralizability of the samples, we also reported the fraction of total post-heating C (mg CO_2-C per mg total C) respired as CO_2 during the entire 12-week incubation (C_{min}, Eq. 4), where $C_{\%}$ is the percentage C for each sample and m_t is the total sample mass for each sample (~ 80 g).

$$C_{\min} = \frac{CO_2\text{–}C}{C_{\%} \cdot 100 \cdot m_t} \tag{4}$$

Fraction of C remaining (C_r) after mineralization was calculated with Eq. 5.

$$C_r = 1 - C_{\min} \tag{5}$$

Modelling mineralizable carbon and carbon decomposition rate

A one-pool decay model (modified from Singh et al. 2012; Eq. 6) was used to fit the values of C_r (Eq. 5) for each treatment using nlsLM function in minpack.lm package in R (Elzhov et al. 2023),

$$C_M = a \cdot e^{-b \cdot t} + (1 - a) \tag{6}$$

where C_M is the modeled fraction of C remaining, coefficient a is the readily decomposable fraction of C, and coefficient b is the decomposition rate (per week), and t is the time (in weeks) after the start of incubation. The first part of the equation represents a typical decay model. Because PyC is so persistent, a simple exponential decay model did not fit the data well, so we added the second term (1-a) to represent the fraction of C that is relatively non-decomposable (over the duration of the incubation).

Statistical analyses

Calculations were performed in Excel and R (R Core Team 2022). A segmented regression model (R Development Core Team 2008) was used to fit the peak temperature as the predictor for pH and identify the temperature associated with the minimum pH value. A two-way ANOVA with an interaction term for heat flux and burial depth, followed by Tukey's HSD test (Tukey 1949; Graves et al. 2019) was used to evaluate treatment effects on pH, total C, mineralized C, DOC, and DIC. A one-way ANOVA followed by Tukey's HSD test (Tukey 1949; Graves et al. 2019) was used to evaluate treatment effects on C mineralizability, decomposable C fraction (coefficient a), and C decomposition rate (coefficient b). Linear models (Oksanen et al. 2022) were used to assess correlations between (1) decomposable C fraction vs. C mineralizability, (2) DOC and DIC vs. pH, and (3) DOC vs. mineralized C. Statistical significance was determined at $p < 0.05$. For some treatments (HF_{High} + Surface and HF_{High} + 1 cm), total remaining C was below detection limits, so these treatments were excluded from analyses of C mineralization and mineralizability. Potential outliers from mineralized C, C mineralizability, and decay model were determined by z-score or iterative z-score and removed from analyses if $|z| > 3$ (3 standard deviations away from the mean). All the figures for visualizing data were made using ggplot2 in R (Wickham 2016).

Heat flux and burial depth were treated as experimental factors in all treatment comparisons. Peak temperature was used only in the segmented regression analysis because the objective of that analysis was to identify the temperature associated with minimum pH, rather than to compare treatment groups.

Results

As heat exposure increased, pH first decreased, then increased

Both HF and burial depth influenced pH ($p < 0.001$, ANOVA in Table S2.1, Tukey's HSD, Fig. 3a), with pH initially decreasing as peak temperature increased, but then increasing as peak temperature reached its highest values (Fig. 3b). Compared to the control, the pH was higher at the surface and at 1 cm under the high heat flux treatment, and lower than the control for the treatments that resulted in intermediate heat exposure (HF_{High} + 5 cm and HF_{Low} + 1 cm). Pyrogenic organic matter was not different from the controls for the low heat flux at the surface and at 5 cm.

The segmented regression model fit the pH vs. peak temperature data relatively well ($R^2 = 0.78$), and indicated that peak temperatures of 273 °C were associated with the lowest pH values (Fig. 3b). Before the breakpoint (273 °C), peak temperature did not affect pH, and after the breakpoint, increasing peak temperatures were associated with increases in pH (Table S2.2 and Text S2.1).

Carbon loss increased with heat flux and decreased with depth, with near-complete combustion at the highest heat exposure

At the same exposure depth, HF_{High} caused more C loss than HF_{Low}, while under the same HF, C loss decreased as burial depth increased (Fig. 4). The C concentrations of HF_{High} + Surface and HF_{High} + 1 cm treatments were below the quantification limit (< 0.05%, Fig. 4), indicating near-complete combustion. Almost all the samples also had N contents below the quantification limit (< 0.03%) except for a few controls, so the data for N concentrations are not presented. In general, both HF and burial depth influenced the C loss of PyOM ($p < 0.001$, ANOVA in Table S3.1, Tukey's HSD, Fig. 4).

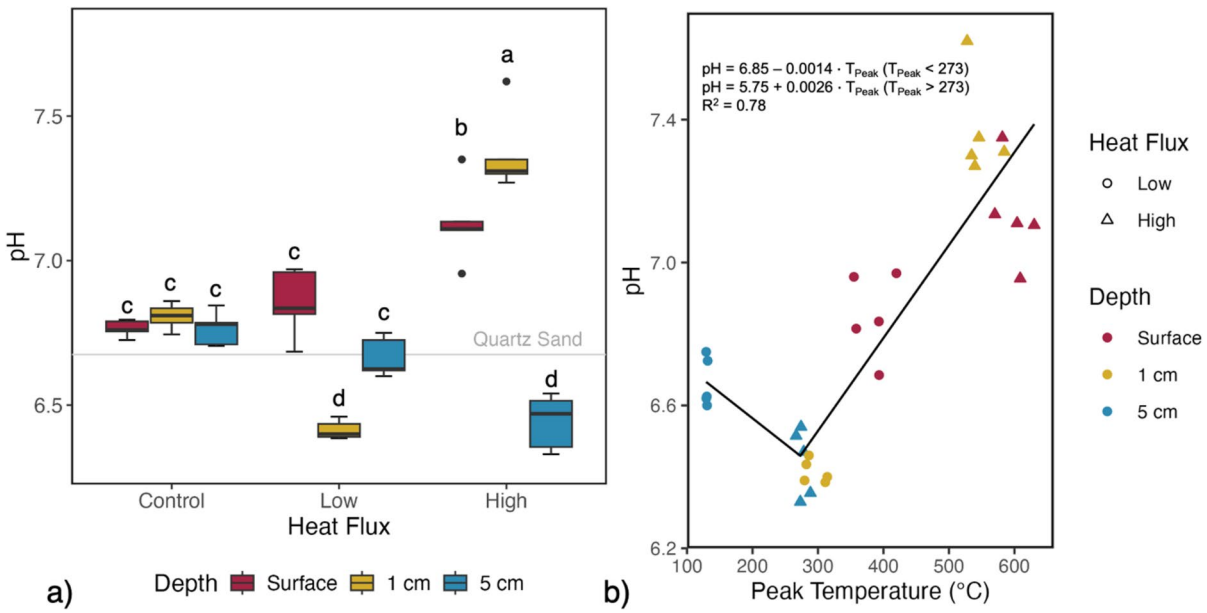


Fig. 3 **a** pH of each treatment (n = 5, $p < 0.001$; grey line indicates pH value of sample blank; letters indicate significant differences; ANOVA, Tukey's HSD). **b** pH vs. the peak temperature of PyOM (lines and equations indicate fits for segmented regression model; $R^2 = 0.78$)

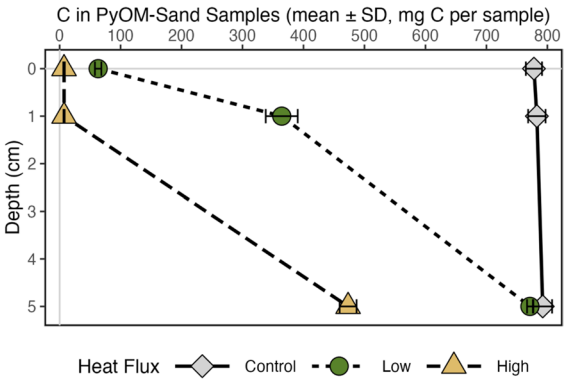


Fig. 4 Mass of C remaining (n = 5, error bars represent ± standard deviation; depth and treatment are both significant, $p < 0.001$; ANOVA)

Intermediate-to-high heat exposure increased PyOM susceptibility to loss via *microbial decomposition after fire*

Counter to our predictions, intermediate heat exposure (HF_{High} + 5 cm and HF_{Low} + 1 cm) generally resulted in the greatest total C mineralization during the 12-week incubation (Fig. 5a) and the highest relative C mineralization rates (on a per g of post-heating C basis; Fig. 5b). These treatments had greater C mineralization than those with low or no heat exposure (HF_{Low} + 5 cm and the controls). Highest heat exposure (HF_{High} + Surface, HF_{High} + 1 cm, and HF_{Low} + Surface) resulted in less C mineralization than HF_{Low} + 5 cm and controls ($p < 0.001$, ANOVA in Table S4.1, Tukey's HSD, Fig. 5a). One sample from the HF_{High} + Surface treatment had extremely high respiration measurements ($z = +5.42$), possibly due to a leak in the jar or sample contamination, and was thus excluded from statistical analyses and figures throughout.

Mineralizability was higher in treatments with intermediate heat exposure (HF_{High} + 5 cm, HF_{Low} + Surface, and HF_{Low} + 1 cm) than HF_{Low} + 5 cm and the controls ($p < 0.001$, ANOVA in Table S5.1, Tukey's HSD, Fig. 5b).

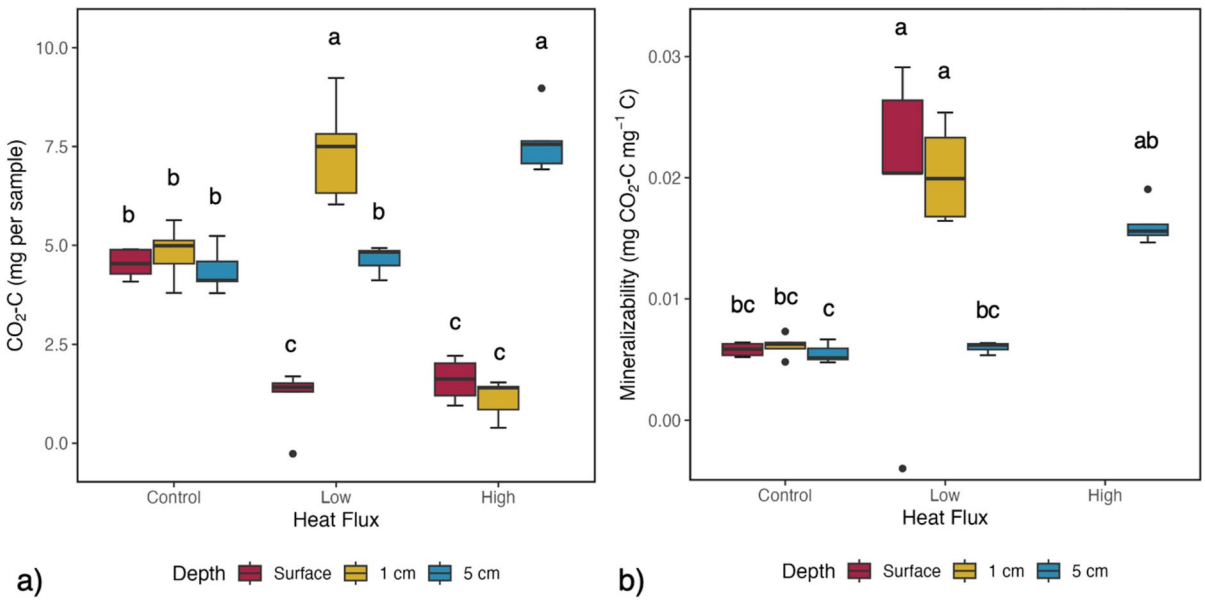


Fig. 5 **a** C loss as CO_2 during 12-week incubation (n = 5; one outlier with a $z = 5.42$ was removed from HF_{High} + Surface; letters indicate significant differences across all treatments: $p < 0.001$; ANOVA, Tukey's HSD); **b** Mineralizability of PyC (n = 5; Treatments HF_{High}+Surface and HF_{High} + 1 cm were excluded due to undetectable amounts of total C; letters indicate significant differences across all treatments: $p < 0.001$; ANOVA, Tukey's HSD)

Higher heat exposure might also lead to increased C mineralizability, but C mineralization per g remaining C could not be calculated because total C was below detection limits.

Over time, CO_2 production generally declined, with most respiration occurring in the first few weeks. Fits for the one-pool decay model of remaining C during the 12-week incubation were good for most of the samples (Fig. S6.1, Table S6.2, R^2 typically > 0.95). We excluded one sample in the HF_{Low} + Surface treatment (Fig. S6.1, top middle panel) because both coefficients in the model were outliers (iterative $z = -3.93$ for coefficient a; iterative $z = 10.30$ for coefficient b), compared to the rest of the samples in the same treatment. This outlier was due to a presumably erroneous negative C mineralization value measured on Week 12.

The readily decomposable C fraction was highest for HF_{Low} + Surface, followed by the intermediate heat exposure treatments (HF_{High} + 5 cm and HF_{Low} + 1 cm), and then HF_{Low} + 5 cm and the controls ($p < 0.001$, ANOVA in Table S6.3, Tukey's HSD, Fig. 6a). This modelled parameter was positively correlated with sample mineralizability (Fig. 6c, Table S6.1). Decomposition rate was higher than controls for HF_{Low} + 1 cm, with small or non-significant differences in all other treatments ($p < 0.001$, ANOVA in Table S6.4, Tukey's HSD, Fig. 6b).

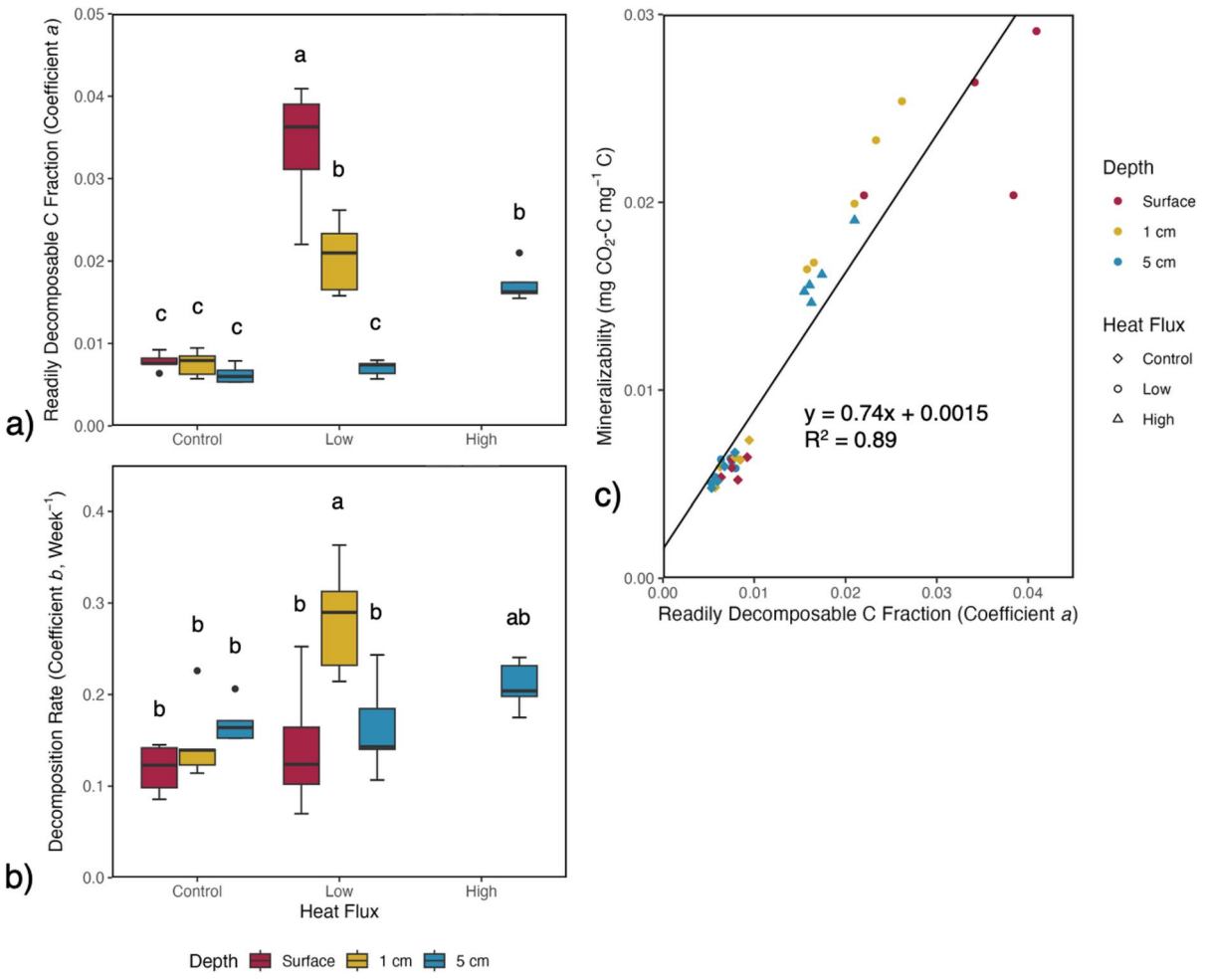


Fig. 6 **a** Readily decomposable C fraction (coefficient a) of the samples from the decay model (n = 5; $p < 0.001$; excluded one outlier in HF_{Low} + Surface); **b** Decomposition rate (coefficient b) of the samples from the decay model (n = 5; $p < 0.001$; excluded one outlier in HF_{Low}+Surface); **c** Mineralizability vs. Readily decomposable C fraction (coefficient a) (line indicates linear fit; $p < 0.001$ for slope; $R^2 = 0.89$)

More DOC is produced from preexisting PyOM after intermediate heat exposure

Dissolved organic carbon increased in treatments with intermediate heat exposure (HF_{High} + 5 cm and HF_{Low} + 1 cm) compared to the controls ($p < 0.001$, ANOVA in Table S7.1, Tukey's HSD, Fig. 7a). For the treatment HF_{Low} + 1 cm, DIC decreased, compared to the controls ($p < 0.001$, ANOVA in Table S7.2, Tukey's HSD, Fig. 7b). In treatments with higher heat exposure (HF_{High} + Surface, HF_{High} + 1 cm, and HF_{Low} + Surface), DOC decreased ($p < 0.001$, ANOVA in Table S7.1, Tukey's HSD, Fig. 7a) while DIC increased ($p < 0.001$, ANOVA in Table S7.2, Tukey's HSD, Fig. 7b).

Dissolved organic carbon was positively correlated with total mineralized C after 12 weeks' incubation ($R^2 = 0.83$, Fig. 8a, Table S7.3). In addition, pH was negatively correlated with DOC concentrations ($R^2 = 0.78$, Fig. 8b, Table S7.4) while it was positively correlated with DIC concentrations ($R^2 = 0.54$, Fig. 8c, Table S7.5).

Discussion

Heating generally increased pH, but intermediate heating decreased pH

In this study, simulated reburn both decreased and increased the pH of PyOM, depending on heat flux and depth. Contrary to our initial hypothesis of a consistent increase, we observed a non-linear pattern. While counter to common assumption that pH inexorably increases with fire, these results are similar to past soil-heating studies (samples that are not PyOM-only): pH decreased after low-temperature heating (150–250 °C) before rising again at higher temperatures (Fernández et al. 1997; Badía and Martí 2003). Our segmented regression model indicated that a peak temperature of 273 °C was associated with the lowest pH (Fig. 3b), which was a little higher than the range reported for soils, suggesting that intermediate heating can produce transient acidification.

The observed transition from acidification to alkalinization may also reflect a progressive shift along the pyrolysis-combustion continuum, during which thermal alteration continuously changes the chemical composition of organic matter (Keiluweit et al. 2010; Doerr et al. 2018). The pH decrease at lower temperatures may be

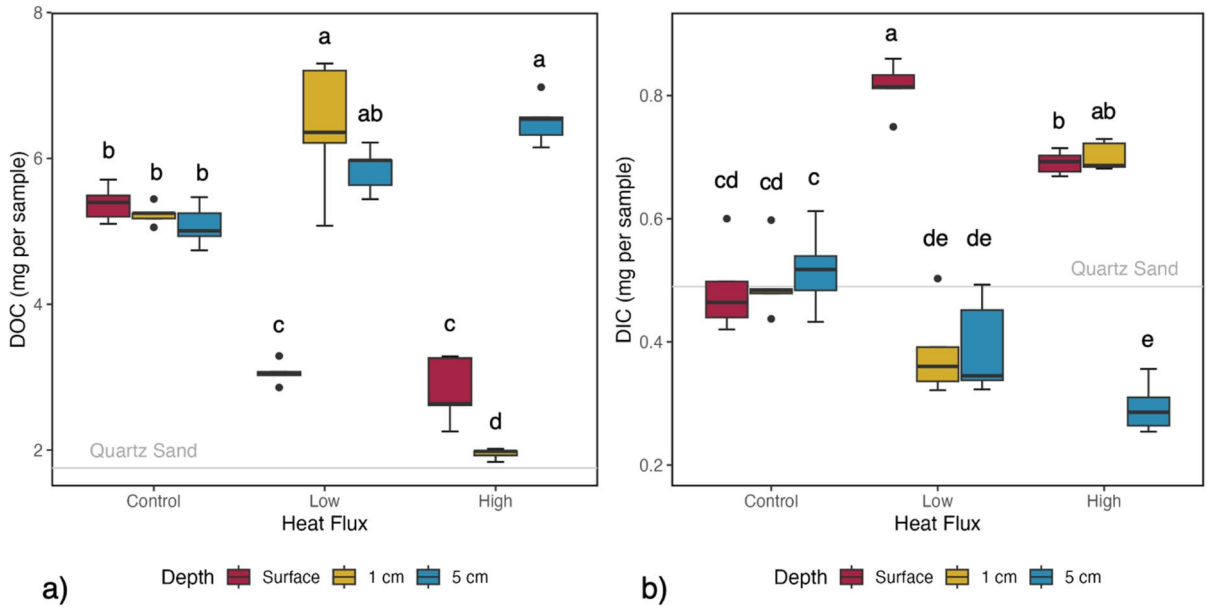


Fig. 7 **a** DOC of samples. Letters indicate significant differences (ANOVA, Tukey's HSD, $p < 0.001$); **b** DIC of samples. Letters indicate significant differences (ANOVA, Tukey's HSD, $p < 0.001$). Grey line indicates sample blank. Mean value for sample blanks with only ground quartz sand is indicated with a grey line

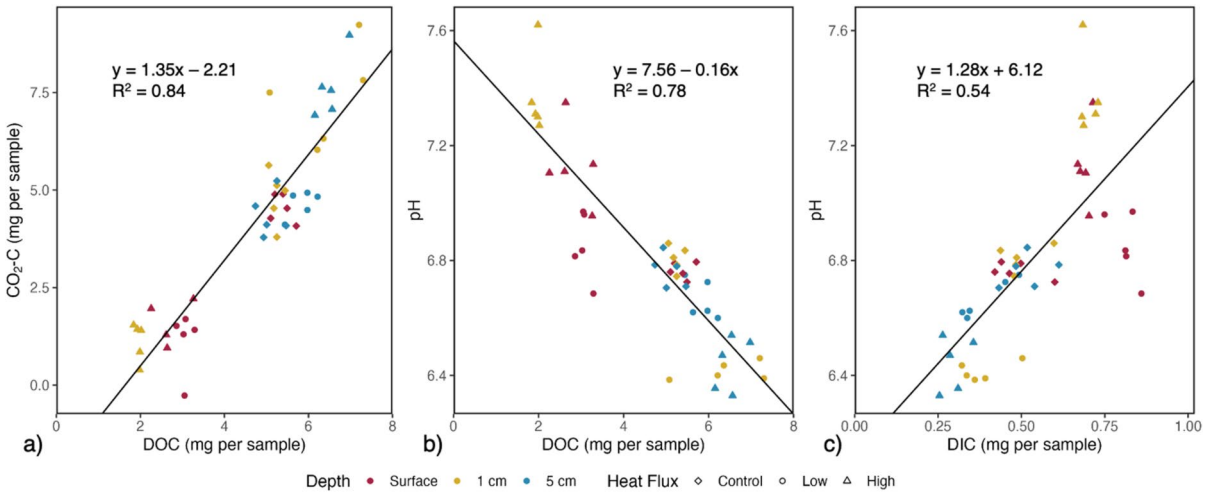


Fig. 8 **a** CO_2-C vs. DOC (line indicates linear fit; $p < 0.001$ for slope and intercept; $R^2 = 0.83$); **b** pH vs. DOC (line indicates linear fit; $p < 0.001$ for slope and intercept; $R^2 = 0.78$); **c** pH vs. DIC (line indicates linear fit; $p < 0.001$ for slope and intercept; $R^2 = 0.54$)

linked to volatilization and condensation of organic acids during heating and subsequent cooling, consistent with our observation that higher DOC coincided with lower pH (Fig. 8b). In contrast, increasing contributions from combustion processes may promote the release of alkaline cations (K^+, Ca^{2+}, and Mg^{2+}) and the loss of proton-donating functional groups, resulting in higher pH values (Badía and Martí 2003; Knicker 2007; Bárcenas-Moreno et al. 2022). This interpretation aligns with the positive correlation observed between pH and DIC, which may reflect the presence of carbonate/bicarbonate ions and associated base cations (Pellegrini et al. 2018). Although pyrolysis and combustion are influenced by both temperature and oxygen availability and likely occurred simultaneously to some extent in our experiment, the minimum pH observed near 273 °C is consistent with a transition from pyrolysis-dominated to increasingly combustion-influenced reactions.

At the lowest heating levels (< 150 °C), we found little change in pH, in agreement with Fernández et al. (1997). However, measurable mass losses (Luo et al. 2025) and C losses indicate that chemical transformations likely still occurred, although not enough to alter pH.

In general, our results reinforce past studies showing that pH does not invariably rise with fire or heating. Instead, intermediate heating can lower pH—a pattern similar to that observed in low-intensity fires and deeper soil horizons. Future studies could explore the full gradient of temperature–pH responses to better constrain local fire heating intensities, and investigate the specific chemistry driving these effects.

Depth and heat flux interact to determine losses of preexisting PyC in the simulated reburn

The self-evident observation that PyOM remains combustible is sometimes overlooked in discussions of its potential role as a C sink in terrestrial ecosystems. However, past studies have clearly reflected this fact: Doerr et al. (2018) found that higher fire intensity caused higher mass and PyC losses, and Tinkham et al. (2016) found that less PyC remained after each reburn. Thus, our findings of PyC losses during the simulated reburn, and more C loss under high heat fluxes do not themselves come as a surprise. Our results are consistent with our hypotheses and past work—for all treatments, we observed C losses, and more C loss occurred under high heat fluxes when the PyOM was at the same depth (Fig. 4).

Perhaps the most important observations from this study are related to the interactions between depth and heat flux. Although many soil heating studies and field measurements have demonstrated that soil temperature declines rapidly with depth during fires (Campbell et al. 1995; Tinkham et al. 2016; McGranahan et al. 2022; Doerr et al.

2025), few studies have explicitly evaluated burial depth as an experimental factor governing the thermal degradation of preexisting PyOM. In our experiment, even at a burial depth of 5 cm, 40.1 ± 1.8% and 2.6 ± 0.6% of total C was lost under High HF and Low HF treatments, respectively (Table S8.1), indicating that burial depth alone does not prevent thermal degradation, but rather interacts strongly with heat flux to determine PyOM persistence.

Regardless, fire-induced C losses are generally expected to decrease with depth because soil heating attenuates rapidly below soil surface (Campbell et al. 1995; Doerr et al. 2025), resulting in greatest—and in some cases, near-complete—losses occurring at and near the surface (Miesel et al. 2015; Xu et al. 2022; Fig. 4; Table S8.1). These findings underscore the critical importance of understanding interactions between changes in fire severity and fire return intervals, and burial rates of PyOM. If PyOM burial/translocation rates are sufficiently high so as to outpace fire return intervals—for example, moving down from O horizon to mineral soil within one year postfire—PyOM is likely to remain protected from losses in subsequent fires (Matosziuk et al. 2020). However, if fire regimes change such that fire frequency increases, or fire severity increases, natural burial rates may become insufficient to preserve preexisting PyOM, resulting in C losses (Doerr et al. 2018; Xu et al. 2022). Similarly, if the mechanisms driving burial rates change (e.g., due to changing precipitation, wind, or sediment deposition rates) (Cotrufo et al. 2016), critical losses in PyOM stocks may occur with future fire regimes. Conversely, if changes in burial rates or fire regimes interact to increase the critical differences between burial rates and fire return intervals or fire severity, then PyOM stocks have the potential to increase (Abney and Berhe 2018). Modelling approaches may be required to help us resolve the range of scenarios expected for a given system or landscape (Foereid et al. 2011).

Subsequent fires may further increase PyC losses through increased mineralizability and DOC production

Previous soil heating studies have shown that heating can alter the availability of mineralizable substrates through thermal transformation of SOM, often producing non-linear responses depending on heating intensity (Choromanska and DeLuca 2002). Contrary to our hypothesis, we found that our simulated reburn increased mineralizability (Fig. 5b) and overall decomposition rate (Fig. 6b)—so much so, that even the total C respired was greater than in the controls (Fig. 5a), despite the reduction in total C remaining in the burned treatments. These results underscore that, at certain burial depths and heat treatments, not only are there direct losses of C due to combustion, but the remaining C is even more susceptible to decomposition, intensifying potential net C losses from the simulated reburn. Choromanska and DeLuca (2002) found that heating increased soluble sugars in soil, which is consistent with our observations of increased DOC and mineralizability, although they were working with soils, not just PyOM. Furthermore, these readily mineralizable fractions may stimulate microbial activity following PyOM addition, potentially through positive priming (stimulation of the decomposition of other SOM) and/or increased nutrient availability associated with ash, thereby diminishing the effects of PyC on C storage after fire (Dungait et al. 2012; Whitman et al. 2014; Maestrini et al. 2015). Mineralized C was positively correlated with, and of a similar magnitude to, total DOC (Fig. 8a). This positive correlation is consistent with past findings that DOC is likely an important contributor to the readily mineralized fraction of the total C that is more readily decomposed by microbes (Zeba et al. 2023).

Although DOC represents a relatively small fraction of total PyC, it is important due to its mineralizability and also its potential translocation (Santos et al. 2022). The release of dissolved PyC occurs slowly over time even when fire is absent (Santos et al. 2017), but dissolved PyC is still thought to account for most of the vertical movement and burial of PyC in mineral soil (Preston and Schmidt 2006; Major et al. 2010). Previous studies have observed that oxidation from fire increases the water solubility of PyC (Preston and Schmidt 2006), and other studies have observed more DOC leached from surface soil with lower-temperature heating (300 °C) than with higher temperatures (450 °C) (Santos et al. 2022), which is consistent with our results. Deep dissolved PyC could form an important part of OM stocks in subsoil horizons, where half of total SOC stocks are located (Rumpel and

Kögel-Knabner 2011), as dissolved PyC can be preferentially transported over other forms of DOC (Soucémarianadin et al. 2019). However, based on our results, in the absence of immediate translocation mechanisms (such as rainfall), the majority of dissolved PyC may instead be mineralized by microbes rapidly after fire.

Experimental limitations

Our experiments did not directly measure the properties of PyOM alone, but, rather, quantified them in the PyOM-sand samples. As discussed in the methods, we expect this methodological decision would generally change the magnitude of some parameters, but not likely the relationships between the treatments. For example, our analyses of burned PyOM used ground samples, which means we neglected potential effects of PyOM particle size that could influence absolute respiration rates. We believe our sampling method effectively recapture the full PyOM samples from the sand, given that the C loss fraction closely mirrored the mass loss fraction (Luo et al. 2025) (Fig. S8.1; Table S8.1; Table S8.2) and that the mass of C in the retrieved control PyOM-sand samples is what we would predict from %C and mass of PyOM alone (Text S8.1). While lab-produced PyOM was the only C source in our experimental system, PyOM is also—to some extent—methodologically defined (see Zimmerman and Mitra 2017). Because we did not use a particular PyOM-quantification method, nor did we directly characterize changes in PyOM chemical composition before or following heating (such as changes in aromaticity, condensation, or other structural characteristics), we cannot distinguish which fractions of PyOM dominated the observed changes in DOC, pH, or respiration. Future work incorporating direct measurements of PyOM structural properties would certainly strengthen mechanistic interpretation of post-reburn changes in PyOM behaviour.

Based on our uninoculated "abiotic incubation", we were unable to conclusively determine how much emitted CO_2 is from inorganic C (Fig. S9.1, Table S9.1). There were leaks in the incubation jars, resulting in the saturation of KOH traps in nearly 1/3 of the samples, and we did not have sufficient PyOM materials to redo the incubation. Despite this limitation, with the remaining measurements, we observe that some of the emitted CO_2 is likely derived from inorganic C (inferred from observed CO_2 emissions from uninoculated samples), but these emissions are consistently less than in the inoculated controls (Fig. 5a and Fig. S9.1). We also recognize that although we do not expect meaningful populations of microbes to exist in the ashed sand and PyOM, the PyOM-sand samples were not actively sterilized, so small populations of existing microbes could have been activated upon the addition of the sterile nutrient solution, also contributing to the CO_2 emissions in the uninoculated control.

Implications for land management and future research

Our results indicate that PyOM combustion is more likely under greater soil heating and when PyOM remains at or near the soil surface. Because soil heating varies substantially among fires and declines rapidly with depth (Doerr et al. 2025), PyOM burial may strongly influence its persistence following subsequent fires. Fire management practices can directly influence the fate of PyOM by affecting both likelihood of combustion and the opportunity for burial between fires.

In general, low-severity fires cause less disturbance to soils (Matosziuk et al. 2019), but may also be associated with higher frequency, and, hence, shorter time for PyOM burial between fires. Fire frequencies that overwhelm PyOM burial rates could thus potentially increase combustion of PyC and decrease long-term accumulation (Preston and Schmidt 2006). Management practices that increase tree and fuel density may elevate the risk of high-severity fires, especially under climate change (Hermoso et al. 2021; Cunningham et al. 2024), thereby increasing the likelihood of PyC losses through deep combustion. Modeling approaches could help predict the net effect of changing fire regimes on soil C and PyC stocks, representing tradeoffs between PyC production and loss rates, as well as the dynamics of non-pyrogenic C.

Although maintaining or elevating soil PyC stocks is rarely an explicit management objective, understanding the factors that influence PyC persistence may help predict long-term PyC fate under different fire regimes. Fire management decisions can influence soil heating through effects on fuel loads and continuity (Keane et al. 2012),

while fire return intervals influence the time available for PyOM burial between successive fires. However, rates and mechanisms of PyOM incorporation into soil remain poorly understood, highlighting a key need for future research across ecosystems and soil types. Because land management objectives often include forest regeneration, wildfire risk mitigation, and habitat restoration, PyC persistence should be considered alongside these broader ecological goals.

Conclusions

Based on the results of our full-factorial experiment with different burial depths of PyOM and different heat flux profiles, we conclude that subsequent fires, or reburns, can not only consume residual PyOM, but also make the remaining PyOM more susceptible to microbial decomposition. We found that high heat flux and/or surface fires (HF_{High} + Surface, HF_{High} + 1 cm, and HF_{Low} + Surface) resulted in large direct C losses through combustion. Intermediate heat exposure (HF_{High} + 5 cm and HF_{Low} + 1 cm) resulted in combustion losses along with increased DOC and mineralizability, which could lead to more complicated long-term effects: increases in the dissolved fraction of PyOM may make it more easily move downward into mineral soil and contribute to the persistent C pool in deep soil, but may also make it more readily decomposable. For the lowest heat flux and deepest burial (HF_{Low} + 5 cm), most PyC was retained, and changes to C mineralization and DOC were minimal. Finally, pH decreased following intermediate heating but increased under higher-temperature heating. Many questions remain regarding how repeated fires will influence PyC dynamics across ecosystems and fire regimes. Future experimental and modeling studies that encompass a broader range of environmental conditions will be necessary to predict the net effect of repeated fires on the global PyC cycle.

Supplementary Information The online version contains supplementary material available at https://doi.org/10.1007/s10533-026-01380-6.

Acknowledgements We would like to thank Roger Bohringer from Wilson State Forest Nursery for the donation of the jack pine tree. We also want to thank Troy Humphrey from Department of Soil and Environmental Sciences for helping cut and grind the tree branches to produce PyOM and Kelsey Kruger for additional support and help.

Author contributions Conceptualization: ML, KY, KB, and TW; Formal analysis: ML; Funding acquisition: TW; Resources: KY, KB, and TW; Supervision: TW; Investigation: ML, KY, and KB; Visualization: ML; Methodology: ML, KY, KB, and TW; Writing—original draft: ML; Writing—review and editing: KY, KB, TW.

Funding This study was funded by the Department of Energy as a part of the project 'Dissection of Carbon and Nitrogen Cycling in Post-Fire Soil Environments using a Genome-Informed Experimental Community' DE-SC0020351. ML was also supported during part of this work by a UW-Madison Hatch grant.

Data availability Data and code associated with this project can be found at https://github.com/MengmengLuo/Fire-removes-preexisting-pyrogenic-organic-matter-from-the-ecosystem and the US Department of Energy ESS-DIVE database as Luo M; Yedinak K; Bourne K; Whitman T (2025): Heating effects on pyrogenic organic matter properties from a pyrocosm study in 2022. Dissection of Carbon and Nitrogen Cycling in Post-Fire Soil Environments using a Genome-Informed Experimental Community (DE-SC0020351). Dataset. https://doi.org/10.15485/3005739.

Declarations

Competing Interests The authors have no relevant financial or non-financial interests to disclose.

Open Access This article is licensed under a Creative Commons Attribution-NonCommercial-NoDerivatives 4.0 International License, which permits any non-commercial use, sharing, distribution and reproduction in any medium or format, as long as you give appropriate credit to the original author(s) and the source, provide a link to the Creative Commons licence, and indicate if you modified the licensed material. You do not have permission under this licence to share adapted material derived from this article or parts of it. The images or other third party material in this article are included in the article's Creative Commons licence, unless indicated otherwise in a credit line to the material. If material is not included in the

article's Creative Commons licence and your intended use is not permitted by statutory regulation or exceeds the permitted use, you will need to obtain permission directly from the copyright holder. To view a copy of this licence, visit http://creativecommons.org/licenses/by-nc-nd/4.0/.

References

Abiven S, Santín C (2019) Editorial: from fires to oceans: dynamics of fire-derived organic matter in terrestrial and aquatic ecosystems. Front Earth Sci 7:31. https://doi.org/10.3389/feart.2019.00031

Abney RB, Berhe AA (2018) Pyrogenic carbon erosion: implications for stock and persistence of pyrogenic carbon in soil. Front Earth Sci 6:26. https://doi.org/10.3389/feart.2018.00026

Abney RB, Jin L, Berhe AA (2019) Soil properties and combustion temperature: controls on the decomposition rate of pyrogenic organic matter. CATENA 182:104127. https://doi.org/10.1016/j.catena.2019.104127

Ansley RJ, Boutton TW, Skjemstad JO (2006) Soil organic carbon and black carbon storage and dynamics under different fire regimes in temperate mixed-grass savanna. Glob Biogeochem Cy 20:1–11. https://doi.org/10.1029/2005gb002670

Badía D, Martí C (2003) Plant ash and heat intensity effects on chemical and physical properties of two contrasting soils. Arid Land Res Manag 17:23–41. https://doi.org/10.1080/15324980301595

Bárcenas-Moreno G, Jiménez-Compán E, Emeterio LMS et al (2022) Soil pH and soluble organic matter shifts exerted by heating affect microbial response. Int J Environ Res Public Health 19:15751. https://doi.org/10.3390/ijerph192315751

Bartoli F, Foderi C, Mastrolonardo G (2021) Effect of repeated burnings, fire and charcoal characteristics on natural charcoal re-combustion in a Mediterranean environment as evaluated in laboratory burning experiments. Geoderma 402:115331. https://doi.org/10.1016/j.geoderma.2021.115331

Berhe AA, Harte J, Harden JW, Torn MS (2007) The significance of the erosion-induced terrestrial carbon sink. Bioscience 57:337–346. https://doi.org/10.1641/b570408

Bird MI, Wynn JG, Saiz G et al (2015) The pyrogenic carbon cycle. Annu Rev Earth Planet Sci 43:1–26. https://doi.org/10.1146/annurev-earth-060614-105038

Boot CM, Haddix M, Paustian K, Cotrufo MF (2014) Distribution of black carbon in Ponderosa pine litter and soils following the high park wildfire. Biogeosci Discuss 11:16799–16824. https://doi.org/10.5194/bgd-11-16799-2014

Bowman DMJS, Balch JK, Artaxo P et al (2009) Fire in the earth system. Science 324:481–484. https://doi.org/10.1126/science.1163886

Bruun S, Jensen ES, Jensen LS (2008) Microbial mineralization and assimilation of black carbon: dependency on degree of thermal alteration. Org Geochem 39:839–845. https://doi.org/10.1016/j.orggeochem.2008.04.020

Campbell GS, Jungbauer JD, Bristow KL, Hungerford RD (1995) Soil temperature and water content beneath a surface fire. Soil Sci 159:363–374. https://doi.org/10.1097/00010694-199506000-00001

Carcaillet C (2001) Are Holocene wood-charcoal fragments stratified in alpine and subalpine soils? Evidence from the Alps based on AMS ^{14}C dates. Holocene 11:231–242. https://doi.org/10.1191/095968301674071040

Certini G (2013) Fire as a soil-forming factor. Ambio 43:191–195. https://doi.org/10.1007/s13280-013-0418-2

Cheng C-H, Lehmann J, Thies JE et al (2006) Oxidation of black carbon by biotic and abiotic processes. Org Geochem 37:1477–1488. https://doi.org/10.1016/j.orggeochem.2006.06.022

Choromanska U, DeLuca TH (2002) Microbial activity and nitrogen mineralization in forest mineral soils following heating: evaluation of post-fire effects. Soil Biol Biochem 34:263–271. https://doi.org/10.1016/s0038-0717(01)00180-8

Coppoletta M, Merriam KE, Collins BM (2016) Post-fire vegetation and fuel development influences fire severity patterns in reburns. Ecol Appl 26:686–699. https://doi.org/10.1890/15-0225

Cotrufo MF, Boot CM, Kampf S et al (2016) Redistribution of pyrogenic carbon from hillslopes to stream corridors following a large montane wildfire. Glob Biogeochem Cycles 30:1348–1355. https://doi.org/10.1002/2016gb005467

Cunningham CX, Williamson GJ, Bowman DMJS (2024) Increasing frequency and intensity of the most extreme wildfires on Earth. Nat Ecol Evol 8:1420–1425. https://doi.org/10.1038/s41559-024-02452-2

DeLuca TH, Aplet GH (2008) Charcoal and carbon storage in forest soils of the Rocky Mountain West. Front Ecol Environ 6:18–24. https://doi.org/10.1890/070070

Doerr SH, Santín C, Merino A et al (2018) Fire as a removal mechanism of pyrogenic carbon from the environment: effects of fire and pyrogenic carbon characteristics. Front Earth Sci 6:127. https://doi.org/10.3389/feart.2018.00127

Doerr SH, Girona-García A, Sanchez-Garcia C et al (2025) Soil heating during wildfires and prescribed burns: a global evaluation. Int J Wildland Fire. https://doi.org/10.1071/wf25103

Dungait JAJ, Hopkins DW, Gregory AS, Whitmore AP (2012) Soil organic matter turnover is governed by accessibility not recalcitrance. Glob Chang Biol 18:1781–1796. https://doi.org/10.1111/j.1365-2486.2012.02665.x

Fernández I, Cabaneiro A, Carballas T (1997) Organic matter changes immediately after a wildfire in an atlantic forest soil and comparison with laboratory soil heating. Soil Biol Biochem 29:1–11. https://doi.org/10.1016/s0038-0717(96)00289-1

Foereid B, Lehmann J, Major J (2011) Modeling black carbon degradation and movement in soil. Plant Soil 345:223–236. https://doi.org/10.1007/s11104-011-0773-3
Forbes MS, Raison RJ, Skjemstad JO (2006) Formation, transformation and transport of black carbon (charcoal) in terrestrial and aquatic ecosystems. Sci Total Environ 370:190–206. https://doi.org/10.1016/j.scitotenv.2006.06.007
Gavin DG (2003) Forest soil disturbance intervals inferred from soil charcoal radiocarbon dates. Can J for Res 33:2514–2518. https://doi.org/10.1139/x03-185
Güereña DT, Lehmann J, Thies JE et al (2015) Partitioning the contributions of biochar properties to enhanced biological nitrogen fixation in common bean (*Phaseolus vulgaris*). Biol Fertil Soils 51:479–491. https://doi.org/10.1007/s00374-014-0990-z
Heitkötter J, Marschner B (2015) Interactive effects of biochar ageing in soils related to feedstock, pyrolysis temperature, and historic charcoal production. Geoderma 245:56–64. https://doi.org/10.1016/j.geoderma.2015.01.012
Hermoso V, Regos A, Morán-Ordóñez A et al (2021) Tree planting: a double-edged sword to fight climate change in an era of megafires. Glob Chang Biol 27:3001–3003. https://doi.org/10.1111/gcb.15625
Hobley E (2019) Vertical distribution of soil pyrogenic matter: a review. Pedosphere 29:137–149. https://doi.org/10.1016/s1002-0160(19)60795-2
Huffman EL, MacDonald LH, Stednick JD (2001) Strength and persistence of fire-induced soil hydrophobicity under ponderosa and lodgepole pine, Colorado Front Range. Hydrol Process 15:2877–2892. https://doi.org/10.1002/hyp.379
Johnson DB, Woolet J, Yedinak KM, Whitman T (2023) Experimentally determined traits shape bacterial community composition one and five years following wildfire. Nat Ecol Evol 7:1419–1431. https://doi.org/10.1038/s41559-023-02135-4
Jones DL, Willett VB (2006) Experimental evaluation of methods to quantify dissolved organic nitrogen (DON) and dissolved organic carbon (DOC) in soil. Soil Biol Biochem 38:991–999. https://doi.org/10.1016/j.soilbio.2005.08.012
Kasin I, Ohlson M (2013) An experimental study of charcoal degradation in a boreal forest. Soil Biol Biochem 65:39–49. https://doi.org/10.1016/j.soilbio.2013.05.005
Keane RE (2012) Describing wildland surface fuel loading for fire management: a review of approaches, methods and systems. Int J Wildland Fire 22:51–62. https://doi.org/10.1071/wf11139
Keiluweit M, Nico PS, Johnson MG, Kleber M (2010) Dynamic molecular structure of plant biomass-derived black carbon (biochar). Environ Sci Technol 44:1247–1253. https://doi.org/10.1021/es9031419
Knicker H (2007) How does fire affect the nature and stability of soil organic nitrogen and carbon? A review. Biogeochemistry 85:91–118. https://doi.org/10.1007/s10533-007-9104-4
Knicker H (2011) Pyrogenic organic matter in soil: its origin and occurrence, its chemistry and survival in soil environments. Quat Int 243:251–263. https://doi.org/10.1016/j.quaint.2011.02.037
Kuzyakov Y, Subbotina I, Chen H et al (2009) Black carbon decomposition and incorporation into soil microbial biomass estimated by 14C labeling. Soil Biol Biochem 41:210–219. https://doi.org/10.1016/j.soilbio.2008.10.016
Leuthold SJ, Soong JL, Even RJ, Cotrufo MF (2025) Decadal persistence of grassland soil organic matter derived from litter and pyrogenic inputs. Nat Geosci 18:226–231. https://doi.org/10.1038/s41561-025-01638-y
Luo M, Yedinak K, Bourne K, Whitman T (2025) Reburning pyrogenic organic matter: a laboratory method for dosing dynamic heat fluxes from above. Int J Wildland Fire 34:WF24128. https://doi.org/10.1071/wf24128
Maestrini B, Nannipieri P, Abiven S (2015) A meta-analysis on pyrogenic organic matter induced priming effect. GCB Bioenergy 7:577–590. https://doi.org/10.1111/gcbb.12194
Major J, Lehmann J, Rondon M, Goodale C (2010) Fate of soil-applied black carbon: downward migration, leaching and soil respiration. Glob Chang Biol 16:1366–1379. https://doi.org/10.1111/j.1365-2486.2009.02044.x
Mansoor S, Farooq I, Kachroo MM et al (2022) Elevation in wildfire frequencies with respect to the climate change. J Environ Manage 301:113769. https://doi.org/10.1016/j.jenvman.2021.113769
Marin-Spiotta E, Chaopricha NT, Plante AF et al (2014) Long-term stabilization of deep soil carbon by fire and burial during early Holocene climate change. Nat Geosci 7:428–432. https://doi.org/10.1038/ngeo2169
Matosziuk LM, Alleau Y, Kerns BK et al (2019) Effects of season and interval of prescribed burns on pyrogenic carbon in ponderosa pine stands in the southern Blue Mountains, Oregon, USA. Geoderma 348:1–11. https://doi.org/10.1016/j.geoderma.2019.04.009
Matosziuk LM, Gallo A, Hatten J et al (2020) Short-term effects of recent fire on the production and translocation of pyrogenic carbon in great smoky mountains national park. Front Global Change 3:6. https://doi.org/10.3389/ffgc.2020.00006
McGranahan DA, Wonkka CL, Dangi S et al (2022) Mineral nitrogen and microbial responses to soil heating in burned grassland. Geoderma 424:116023. https://doi.org/10.1016/j.geoderma.2022.116023
Miesel JR, Hockaday WC, Kolka RK, Townsend PA (2015) Soil organic matter composition and quality across fire severity gradients in coniferous and deciduous forests of the southern boreal region. J Geophys Res Biogeosci 120:1124–1141. https://doi.org/10.1002/2015jg002959
Nikolakis W, Roberts E (2020) Indigenous fire management: a conceptual model from literature. Ecol Soc. https://doi.org/10.5751/es-11945-250411
Ohlson M, Dahlberg B, Økland T et al (2009) The charcoal carbon pool in boreal forest soils. Nat Geosci 2:692–695. https://doi.org/10.1038/ngeo617

Pellegrini AFA, Ahlström A, Hobbie SE et al (2018) Fire frequency drives decadal changes in soil carbon and nitrogen and ecosystem productivity. Nature 553:194–198. https://doi.org/10.1038/nature24668
Pingree MRA, DeLuca TH (2017) Function of wildfire-deposited pyrogenic carbon in terrestrial ecosystems. Front Environ Sci 5:53. https://doi.org/10.3389/fenvs.2017.00053
Preston CM, Schmidt MWI (2006) Black (pyrogenic) carbon: a synthesis of current knowledge and uncertainties with special consideration of boreal regions. Biogeosciences 3:397–420. https://doi.org/10.5194/bg-3-397-2006
Radeloff VC, Mladenoff DJ, Guries RP, Boyce MS (2004) Spatial patterns of cone serotiny in *Pinus banksiana* in relation to fire disturbance. Forest Ecol Manag 189:133–141. https://doi.org/10.1016/j.foreco.2003.07.040
Rumpel C, Kögel-Knabner I (2011) Deep soil organic matter—a key but poorly understood component of terrestrial C cycle. Plant Soil 338:143–158. https://doi.org/10.1007/s11104-010-0391-5
Saberi SJ, Harvey BJ (2023) What is the color when black is burned? Quantifying (re)burn severity using field and satellite remote sensing indices. Fire Ecol 19:24. https://doi.org/10.1186/s42408-023-00178-3
Santín C, Doerr SH, Preston C, Bryant R (2013) Consumption of residual pyrogenic carbon by wildfire. Int J Wildland Fire 22:1072–1077. https://doi.org/10.1071/wf12190
Santín C, Doerr SH, Preston CM, González-Rodríguez G (2015) Pyrogenic organic matter production from wildfires: a missing sink in the global carbon cycle. Glob Change Biol 21:1621–1633. https://doi.org/10.1111/gcb.12800
Santín C, Doerr SH, Kane ES et al (2016) Towards a global assessment of pyrogenic carbon from vegetation fires. Glob Change Biol 22:76–91. https://doi.org/10.1111/gcb.12985
Santos F, Torn MS, Bird JA (2012) Biological degradation of pyrogenic organic matter in temperate forest soils. Soil Biol Biochem 51:115–124. https://doi.org/10.1016/j.soilbio.2012.04.005
Santos F, Wagner S, Rothstein D et al (2017) Impact of a historical fire event on pyrogenic carbon stocks and dissolved pyrogenic carbon in Spodosols in northern Michigan. Front Earth Sci 5:80. https://doi.org/10.3389/feart.2017.00080
Santos F, Bird JA, Berhe AA (2022) Dissolved pyrogenic carbon leaching in soil: effects of soil depth and pyrolysis temperature. Geoderma 424:116011. https://doi.org/10.1016/j.geoderma.2022.116011
da Silva LJ, da Oliveira SDM, Nóbrega GN et al (2023) Pyrogenic carbon stocks and its spatial variability in soils from savanna-forest ecotone in amazon. J Environ Manag 340:117980. https://doi.org/10.1016/j.jenvman.2023.117980
Simonson RW (1959) Outline of a generalized theory of soil genesis. Soil Sci Soc Am J 23:152–156. https://doi.org/10.2136/sssaj1959.03615995002300020021x
Singh N, Abiven S, Torn MS, Schmidt MWI (2012) Fire-derived organic carbon in soil turns over on a centennial scale. Biogeosciences 9:2847–2857. https://doi.org/10.5194/bg-9-2847-2012
Sokol NW, Slessarev E, Marschmann GL et al (2022) Life and death in the soil microbiome: how ecological processes influence biogeochemistry. Nat Rev Microbiol 20:1–16. https://doi.org/10.1038/s41579-022-00695-z
Soong JL, Cotrufo MF (2015) Annual burning of a tallgrass prairie inhibits C and N cycling in soil, increasing recalcitrant pyrogenic organic matter storage while reducing N availability. Glob Chang Biol 21:2321–2333. https://doi.org/10.1111/gcb.12832
Soucémarianadin L, Reisser M, Cécillon L et al (2019) Pyrogenic carbon content and dynamics in top and subsoil of French forests. Soil Biol Biochem 133:12–15. https://doi.org/10.1016/j.soilbio.2019.02.013
Spokas KA (2010) Review of the stability of biochar in soils: predictability of O:C molar ratios. Carbon Manag 1:289–303. https://doi.org/10.4155/cmt.10.32
Strotmann U, Reuschenbach P, Schwarz H, Pagga U (2004) Development and evaluation of an online CO_2 evolution test and a multicomponent biodegradation test system. Appl Environ Microb 70:4621–4628. https://doi.org/10.1128/aem.70.8.4621-4628.2004
Tinkham WT, Smith AMS, Higuera PE et al (2016) Replacing time with space: using laboratory fires to explore the effects of repeated burning on black carbon degradation. Int J Wildland Fire 25:242–248. https://doi.org/10.1071/wf15131
Tinner W, Hofstetter S, Zeugin F et al (2006) Long-distance transport of macroscopic charcoal by an intensive crown fire in the Swiss Alps - implications for fire history reconstruction. Holocene 16:287–292. https://doi.org/10.1191/0959683606hl925rr
Tukey JW (1949) Comparing individual means in the analysis of variance. Biometrics 5(2):99. https://doi.org/10.2307/3001913
Westerling AL, Hidalgo HG, Cayan DR, Swetnam TW (2006) Warming and earlier spring increase Western U.S. forest wildfire activity. Science 313:940–943. https://doi.org/10.1126/science.1128834
Whitman T, Hanley K, Enders A, Lehmann J (2013) Predicting pyrogenic organic matter mineralization from its initial properties and implications for carbon management. Org Geochem 64:76–83. https://doi.org/10.1016/j.orggeochem.2013.09.006
Whitman T, Zhu Z, Lehmann J (2014) Carbon mineralizability determines interactive effects on mineralization of pyrogenic organic matter and soil organic carbon. Environ Sci Technol 48:13727–13734. https://doi.org/10.1021/es503331y
Whitman T, Fang Y, Luo Y (2026) Chapter 17: Biochar effects on soil carbon turnover. In: Lehmann J, Joseph S (eds) Biochar for Environmental Management Science, Technology and Implementation. Routledge, London, UK

Wickham H (2016) Ggplot2: elegant graphics for data analysis. Springer-Verlag, New York. https://doi.org/10.1007/978-3-319-24277-4_9
Xiao F (2022) A review of biochar functionalized by thermal air oxidation. Environ Funct Mater 1:187–195. https://doi.org/10.1016/j.efmat.2022.03.001
Xu S, Eisenhauer N, Pellegrini AFA et al (2022) Fire frequency and type regulate the response of soil carbon cycling and storage to fire across soil depths and ecosystems: a meta-analysis. Sci Total Environ 825:153921. https://doi.org/10.1016/j.scitotenv.2022.153921
Zeba N, Berry TD, Panke-Buisse K, Whitman T (2022) Effects of physical, chemical, and biological ageing on the mineralization of pine wood biochar by a *Streptomyces* isolate. PLoS One 17:e0265663. https://doi.org/10.1371/journal.pone.0265663
Zeba N, Berry TD, Fischer MS, Traxler MF, Whitman T (2023) Soil carbon mineralization and microbial community dynamics in response to PyOM addition. bioRxiv. https://doi.org/10.1101/2023.06.21.545992
Zimmerman AR, Mitra S (2017) Trial by fire: on the terminology and methods used in pyrogenic organic carbon research. Front Earth Sci 5:95. https://doi.org/10.3389/feart.2017.00095
Elzhov TV, Mullen KM, Spiess A, Bolker B (2023) minpack.lm: R interface to the Levenberg-Marquardt nonlinear least-squares algorithm found in MINPACK, plus support for bounds. R package. https://CRAN.R-project.org/package=minpack.lm
Graves S, Piepho H, Dorai-Raj S (2019) multcompView: Visualizations of paired comparisons. R package. https://CRAN.R-project.org/package=multcompView
Hofmann D, Steffen D, Jablonowski ND, Burauel P (2012) Dissolved organic carbon (DOC) in soil extracts investigated by FT-ICR-MS. EGU General Assembly abstract. Retrieved from https://ui.adsabs.harvard.edu/abs/2012EGUGA..14139 57H/abstract
National Instruments (2013) LabVIEW, version 2013. National Instruments, Austin, TX, USA. https://www.ni.com/en-us/shop/labview.html
Oksanen J, Simpson G, Blanchet F, et al (2022) vegan: Community ecology package. R package. https://CRAN.R-project.org/package=vegan
R Core Team (2022) R: A language and environment for statistical computing. R Foundation for Statistical Computing, Vienna, Austria. https://www.R-project.org/
R Development Core Team (2008) R: A language and environment for statistical computing. R Foundation for Statistical Computing. http://cran.r-project.org/doc/Rnews/Rnews_2008-1.pdf
Schindelbeck R, Moebius-Clune D, Kurtz K, et al (2016) Cornell Soil Health Laboratory comprehensive assessment of soil health standard operating procedures. https://cpb-us-e1.wpmucdn.com/blogs.cornell.edu/dist/f/5772/files/2015/03/CASH-Standard-Operating-Procedures-030217final-u8hmwf.pdf

Publisher's Note Springer Nature remains neutral with regard to jurisdictional claims in published maps and institutional affiliations.

Authors and Affiliations

Mengmeng Luo[1] · Kara Yedinak[2] · Keith Bourne[3] · Thea Whitman[1,4]

✉ Thea Whitman
twhitman@wisc.edu

[1] Department of Soil and Environmental Sciences, College of Agricultural and Life Sciences, University of Wisconsin-Madison, 1525 Observatory Drive, Madison, WI 53706, USA

[2] Northern Research Station, USDA Forest Service, 1 Gifford Pinchot Drive, Madison, WI 53726, USA

[3] Forest Products Laboratory, USDA Forest Service, 1 Gifford Pinchot Drive, Madison, WI 53726, USA

[4] Department of Microbiology and Immunology, University of British Columbia, 2350 Health Sciences Mall, Vancouver, BC V6T 1Z3, Canada